



Delft University of Technology

## Occupancy-based demand response and thermal comfort optimization in microgrids with renewable energy sources and energy storage

Korkas, C; Baldi, S; Michailidis, I; Kosmatopoulos, EB

### DOI

[10.1016/j.apenergy.2015.10.140](https://doi.org/10.1016/j.apenergy.2015.10.140)

### Publication date

2016

### Document Version

Accepted author manuscript

### Published in

Applied Energy

### Citation (APA)

Korkas, C., Baldi, S., Michailidis, I., & Kosmatopoulos, EB. (2016). Occupancy-based demand response and thermal comfort optimization in microgrids with renewable energy sources and energy storage. *Applied Energy*, 163, 93-104. <https://doi.org/10.1016/j.apenergy.2015.10.140>

### Important note

To cite this publication, please use the final published version (if applicable). Please check the document version above.

### Copyright

Other than for strictly personal use, it is not permitted to download, forward or distribute the text or part of it, without the consent of the author(s) and/or copyright holder(s), unless the work is under an open content license such as Creative Commons.

### Takedown policy

Please contact us and provide details if you believe this document breaches copyrights. We will remove access to the work immediately and investigate your claim.

# Occupancy-based Demand Response and Thermal Comfort Optimization in Microgrids with Renewable Energy Sources and Energy Storage

Christos D. Korkas<sup>a,c,\*</sup>, Simone Baldi<sup>b</sup>, Iakovos Michailidis<sup>a,c</sup>, Elias B. Kosmatopoulos<sup>a,c</sup>

<sup>a</sup> Dept. of Electrical and Computer Engineering, Democritus University of Thrace, Xanthi 67100, Greece

<sup>b</sup> Delft Center for Systems and Control, Delft University of Technology, Delft 2628CD, The Netherlands

<sup>c</sup> Informatics & Telematics Institute, Center for Research and Technology Hellas (ITI-CERTH), Thessaloniki 57001, Greece

---

## Abstract

Integration of renewable energy sources in microgrids can be achieved via demand response programs, which change the electric usage in response to changes in the availability and price of electricity over time. This paper presents a novel control algorithm for joint demand response management and thermal comfort optimization in microgrids equipped with renewable energy sources and energy storage units. The proposed work aims at covering two main gaps in current state-of-the-art demand response programs. The first gap is integrating the objective of matching energy generation and consumption with the occupant behavior and with the objective of guaranteeing thermal comfort of the occupants. The second gap is developing a scalable and robust demand response program. Large-scale nature of the optimization problem and robustness are achieved via a two-level supervisory closed-loop feedback strategy: at the lower level, each building of the microgrid employs a local closed-loop feedback controller that processes only local measurements; at the upper level, a centralized unit supervises and updates the local controllers with the aim of minimizing the aggregate energy cost and thermal discomfort of the microgrid. The effectiveness of the proposed method is validated in a microgrid composed of three buildings, a photovoltaic array, a wind turbine, and an energy storage unit. Comparisons with alternative demand response strategies reveal that the proposed strategy efficiently integrates the renewable sources; energy costs are reduced and at the same time thermal comfort of the occupants is guaranteed. Furthermore, robustness is proved via consistent improvements achieved under heterogeneous conditions (different occupancy schedules and different weather conditions).

**Keywords:** Demand response, Microgrid, Thermal comfort optimization, Occupancy information

---

## 1. Introduction

Increasing energy demand and stricter environmental regulations are promoting the transition from traditional electric grids with centralized power plants to smart electrical microgrids where the existing power grid is enhanced by distributed, small-scale, renewable-energy generation systems such as photovoltaic panels, wind turbines, and energy storage units [1]. Microgrids can be seen as miniature versions of the larger utility grid except that, when necessary, they can disconnect from the main grid and can continue to operate in ‘islanded mode’ [2]. Despite their potential advantages, a main challenge needs to be overcome: the

---

\*Corresponding author. Tel.: +30 2541 551597

Email addresses: ckorkas@ee.duth.gr (Christos D. Korkas), s.baldi@tudelft.nl (Simone Baldi), michailid@iti.gr (Iakovos Michailidis), kosmatop@iti.gr (Elias B. Kosmatopoulos)

33 widespread availability of renewable sources inserts uncertainty into the grid, due to their stochastic out-  
34 put profile which strongly depends on local weather conditions. Lack of monitoring and control of these  
35 energy sources might contribute to the instability of the electric grid: this is especially true in grids where  
36 fluctuating power may be delivered due to the high participation of renewable energy sources [3]. Energy  
37 storage systems play a central role in the integration of renewable energy sources in microgrids, as they  
38 provide the necessary flexibility to compensate unbalances between the power supply and the demand. The  
39 interesting experimental work in [4] assesses how the timing of an electric outage affects the islanding life-  
40 time of a microgrid, with and without energy storage. For these reasons, one of the pivotal questions in the  
41 widespread diffusion of microgrids is to deploy a control system which will take the appropriate decisions  
42 for the energy distribution and consumption, in order to minimize the energy consumption and cost: this  
43 task goes under the name of ‘demand response’ [5].

44 Demand response requires the development of control mechanisms that can autonomously facilitate  
45 changes in electric usage by end-use customers in response to changes in the price of electricity over time, or  
46 in response to the availability of renewable energy [6]. The implementation of these mechanisms require the  
47 presence of loads whose operation can be regulated, i.e. controllable loads. Many studies show that HVAC  
48 operations account for nearly 50% of the energy consumed by a building [7]: furthermore, good HVAC  
49 control is one of the most cost-effective option to implement demand response and improve the energy  
50 efficiency of microgrids. For example, it has been shown that raising summer set point temperature might  
51 have good and universal energy saving potential as it can be applied to both new and existing buildings [8].  
52 However, HVAC operation cannot aim exclusively at energy savings without taking into account the effect of  
53 changing the control strategy on indoor comfort: the ASHRAE55 and EN15251 standards [9, 10] pose strict  
54 constraints on the end-user (building occupant) thermal comfort, with bounds and constraints that should  
55 not be violated except for small intervals during the building operation. The literature on demand response  
56 with thermal comfort optimization is vast: without aiming at being comprehensive, in the following we give  
57 a brief overview on the topic.

### 58 *1.1. State-of-the-art in demand response with thermal comfort*

59 As a large portion of building energy consumption is used for thermal comfort, optimization of energy  
60 and comfort calls for delicate trade-offs, which have been studied by many researchers: the simulation tool  
61 of [11] can predict the effect of changing the control strategy on indoor comfort and energy consumption.  
62 The authors of [12] develop control strategies for intelligent glazed facades and investigate the influence  
63 of different control strategies on energy and comfort performance in office buildings. Particle swarm opti-  
64 mization has been applied in [13] to optimize the set points based on the comfort zone. In [14] the operation  
65 of variable air volume air conditioning is optimized with respect to comfort and indoor air quality. The  
66 influence on energy consumption of thermostat operation and thermal comfort requirements is the object of  
67 the study in [15]. All this approaches show, sometimes also via real-life experiments, that relevant energy  
68 savings can be achieved without compromising thermal comfort.

69 The use of occupancy information plays a major role in decreasing energy costs and improving thermal  
70 comfort: the potential of using occupancy information in model predictive-based building climate control is  
71 investigated in [16]. The approach of [17] aligns the distribution of residents’ thermostat preferences with  
72 the indoor temperature to maximize thermal comfort while reducing energy savings. Using the expected  
73 room occupancy schedule, the evolutionary algorithm of [18] produces optimized ventilation strategies with  
74 reduced CO<sub>2</sub> concentration and energy costs. The goal of [19] is to use occupancy information to reduce  
75 energy use while maintaining thermal comfort and indoor air quality.

76 Multi-objective optimization of energy consumption and thermal comfort is well established at the  
77 building level: at the microgrid level, however, most state-of-the-art microgrid energy management systems

78 aiming at improving resilience and enabling islanded mode, consider only matching energy generation  
79 and consumption [20, 21, 22]: other multi-objective optimization examples include optimize the power  
80 dispatch of the microgrid according to economy and reliability interests of the power grid [23], decreasing  
81 the expenses for power purchase or increasing revenues from power selling [24]. Operational results of  
82 real-life microgrids have also been provided [25, 26, 27]. However, in the aforementioned works and  
83 experimental evaluations, thermal comfort of the occupants is often neglected, or, when considered, it is  
84 oversimplified. A typical oversimplification involves considering bounds on the dry-bulb temperature [28]:  
85 this is a poor comfort-maintaining criterion, since neglecting humidity and radiant temperatures can lead to  
86 insufficient estimation of actual thermal comfort. The Fanger index [9] or adaptive thermal comfort models  
87 [29] can yield a realistic estimate of thermal comfort. Summarizing, to the best of the authors' knowledge  
88 the following gaps can be identified in the state of the art of demand response in microgrids:

89 G1) *Thermal and occupancy information in microgrids*: a part from some recent contributions by the  
90 authors [30], there is no demand response program at the microgrid level that can exploit occupancy  
91 information with the objective of guaranteeing thermal comfort of the occupants. Note that the work  
92 in [30] do not consider the presence of multiple renewable energy sources (possibly with different  
93 prices) and of energy storage.

94 G2) *Scalability to large microgrids*: there is no demand response program that can be scalable to large-  
95 scale microgrids: also the recent work in [19] considers a centralized architecture stemming informa-  
96 tion from the entire microgrid: this might be impractical in microgrids of large dimension.

97 G3) *Robustness of solution*: there is no real study on robustness of demand response programs in front  
98 of changing conditions, including changing occupancy patterns and changing weather conditions:  
99 due to the computational complexity of predictive control strategies, most of the cited state-of-the-art  
100 demand response are tested over relatively short horizons, and it is not clear whether they can achieve  
101 consistent improvements over longer ones. Furthermore, their predictive control nature requires the  
102 optimization task to be continuously active: it is not clear whether it is possible to develop a demand  
103 response program that, after optimization over a short horizon, can be used over longer horizons with  
104 consistent improvements.

105 With this work we try to cover the identified gaps in demand response and thermal comfort optimization in  
106 microgrids, as explained hereafter.

## 107 1.2. Main contributions of the work

108 This paper presents a novel control algorithm for joint demand response management and thermal com-  
109 fort optimization in microgrids equipped with renewable energy sources and energy storage. With respect  
110 to the three identified gaps, the work provides the following contributions:

111 C1) *Thermal and occupancy information in microgrids*: demand response is achieved by controlling  
112 the HVAC system of each building: the final objective is not only the reduction of the energy ab-  
113 sorbed from the traditional electrical grid, but also guaranteeing acceptable thermal comfort con-  
114 ditions. The Fanger index is used as a realistic measure for thermal comfort. The proposed sys-  
115 tem uses a simulation-based optimization procedure: together with Model Predictive Control (MPC)  
116 [31, 32, 33, 34], simulation-based optimization is emerging as a strategy for energy-efficient control  
117 and smart grids [35, 36, 37, 38]. The proposed demand response program is a parametrized feedback  
118 control strategy where the parameters are dependent on the thermal state of the buildings, but also  
119 on the occupancy pattern of the microgrid : this will lead to efficient exploitation of the occupancy  
120 information stemming from the microgrid.

121 C2) *Scalability to large microgrids*: from the control perspective, a microgrid is a large-scale dynamic  
122 system with high complexity and a huge amount of information. Proper combination of the available  
123 information and effective control of the overall microgrid system turns out to be a big challenge [39].  
124 In order to address the computational complexity, the proposed control strategy adopt a two-level  
125 supervisory strategy: at the lower level, each building employs a local controller that processes only  
126 local measurements; at the upper level, a centralized unit supervises and updates the three controllers  
127 with the aim of minimizing the aggregate energy cost and thermal discomfort of the microgrid. This  
128 distributed architecture is supposed to be scalable to microgrids composed of many buildings.

129 C3) *Robustness of solution*: simulation-based optimization allows the use of elaborate microgrid mod-  
130 els (built via simulation tools like EnergyPlus, TRNSYS, Modelica etc. [40, 41]): an advantage  
131 is that reliable simulations over long horizons can be conducted in order to address the large-scale  
132 complexity and the real-time requirements. The parametrized demand response strategy developed  
133 in this work will be used to test to what extent a demand response program optimized over short  
134 horizons can be robust when implemented over long horizons: it will be verified that the proposed  
135 demand response program, due to its feedback nature employing thermal and occupancy information,  
136 achieves consistent improvements in front of changing conditions, including changing occupancy  
137 patterns and changing weather conditions. This is a relevant achievement in terms of required com-  
138 putational complexity, as it shows that optimization does not have to be carried out continuously but,  
139 after optimization over a short horizon, the proposed demand response program can be used over  
140 longer horizons with consistent improvements.

141 A test case consisting of a microgrid with three buildings connected to a photovoltaic array, a wind turbine,  
142 an energy storage and to the traditional electrical grid is used to evaluate the effectiveness of the proposed  
143 algorithm. Comparisons with alternative demand response strategies reveal that the proposed supervisory  
144 strategy efficiently handles the large-scale of the optimization problem, manages the demand response so  
145 as to sensibly improve independence of the microgrid with respect to the main grid, and guarantees at the  
146 same time thermal comfort of the occupants.

147 The paper is organized as follows: Section II describes the problem setting, the microgrid and its at-  
148 tributes. Section III deals with the control objectives and the performance index. In Section IV the su-  
149 pervisory control architecture is presented, while Section V presents the PCAO algorithm used for the  
150 optimization problem. Section VI presents the results and Section VII concludes the paper.

## 151 2. Problem description

152 In this section we present the setting of the joint demand response management and thermal comfort  
153 optimization problem. A grid-connected microgrid, shown in Figure 1, is composed of three buildings  
154 and equipped with renewable energy sources (photovoltaic panels and wind turbines) and a shared energy  
155 storage unit for electricity. The grid is also connected to the main electricity grid. In order to fulfill their  
156 energy needs, the buildings of the microgrid share the energy sources and the stored energy in a common  
157 pool: the renewable energy sources are so-called ‘must-take’ sources, where their output is always used  
158 when it is available. If the output of the renewable energy sources is not enough, the extra electricity is  
159 absorbed for the main grid. In the following, more details about the different components of the microgrid  
160 are given.

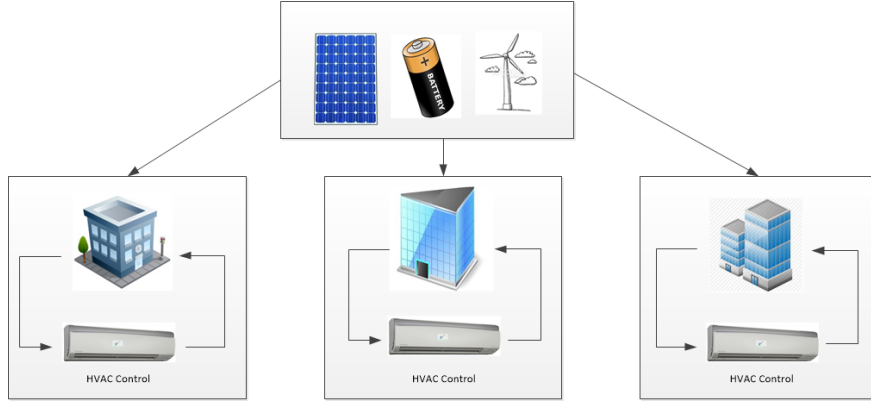


Figure 1: Supervisory Control Strategy

Table 1: Microgrid description

	No. of Thermal Zones	Size	Use
Building 1	10 thermal zones	500 $m^2$	Industrial
Building 2	10 thermal zones	900 $m^2$	Commercial
Building 3	10 thermal zones	300 $m^2$	Residential

161 *2.1. Controllable and uncontrollable loads*

162 Table 1 shows the composition of the microgrid: the three buildings cover a surface of 500  $m^2$ , 900  $m^2$   
 163 and 300  $m^2$ , respectively. In order to consider a heterogeneous microgrid scenario with different occupancy  
 164 patterns, we assume that the buildings are of commercial, industrial and residential type, respectively. Each  
 165 building has two floors and ten thermal zones. Each thermal zone is equipped with an HVAC unit, where  
 166 every HVAC unit is opportunely dimensioned according to the size of the thermal zone. This results in a  
 167 scenario where each building has different energetic needs. The HVAC are operated via temperature set  
 168 points, one for each unit: by regulating the thirty set points, part of the energy demand of the microgrid  
 169 is controlled. In our setting HVACs are the only controllable loads of the microgrid: this is based on  
 170 the fact that HVAC operation accounts for nearly 50% of the energy consumed by a building and on the  
 171 hypothesis that the other types of loads of the microgrid (lighting, industrial machines, PCs, etc.) are  
 172 not responsive and cannot be curtailed [42]. Uncontrollable loads account for the not responsive part of the  
 173 energy consumption: three load daily profiles, shown in Figure 2 have been created based on typical profiles  
 174 of commercial, industrial and residential consumers [43, 44, 45].

175 *2.2. Occupancy schedule*

176 In order to make the joint demand response and thermal comfort optimization tasks more challenging,  
 177 the three buildings are assumed to have different occupancy schedules, which are shown in Table 2. Roughly  
 178 speaking, when the three buildings of the microgrid have a different occupancy schedule, the demand re-  
 179 sponse program should be able to switch off the HVACs of a building when no occupants are there, in order  
 180 to allow the other buildings to use the available renewable energy. The different occupancy schedules arise  
 181 from the different use of each building. In particular, the first building is assumed to host industrial activi-  
 182 ties and the second building is used as an office; the third building exhibits a possible residential occupancy

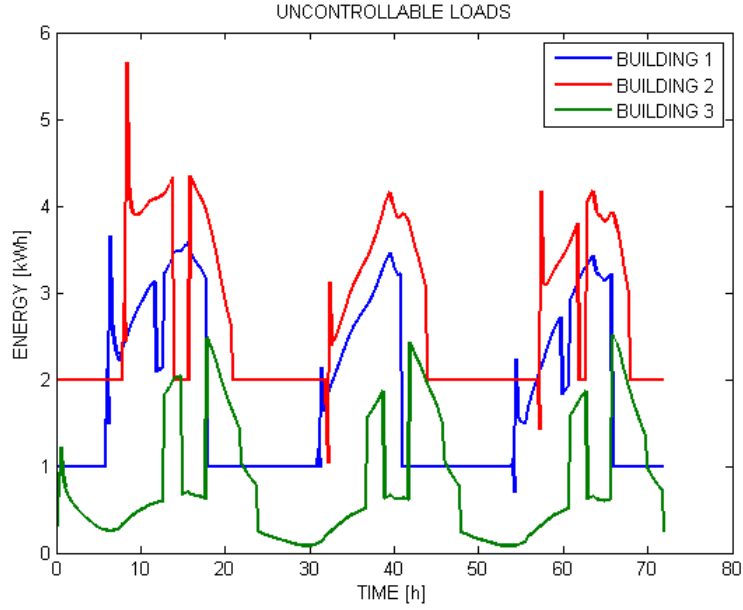


Figure 2: Uncontrollable loads of the three buildings over three days

183 schedule. The schedule of Table 2 has been designed in such a way that a variety of situations occur. Some-  
 184 times all three buildings are occupied and, other times, only one building is occupied. It is assumed that all  
 185 the thermal zones of a building exhibit the same occupancy pattern.

Table 2: Occupancy Schedule

	Day 1	Day 2	Day 3
Building 1	6am - 12am and 13pm - 18pm	7am - 17pm	6am - 12am and 13pm - 18pm
Building 2	8am - 14pm and 16pm - 21pm	8am - 20pm	9am - 14pm and 15pm - 20pm
Building 3	0am - 24pm	0am - 24pm	0am - 24pm

### 186 2.3. Renewable energy sources

187 The energy from the renewable sources comes with a different price, as shown in Table 3: the different  
 188 prices account for the fact that producing solar energy costs differently than producing wind energy [46, 47].  
 189 Furthermore, the prices of the electricity generated by renewable energy includes also investment costs and  
 190 maintenance costs of resources [48]. Because of the different prices, the energy is absorbed in the following  
 191 order: wind, solar, storage, main grid. The energy is drained proportionally to the energy demand of each  
 192 building of the microgrid according to the Kirchhoff's circuit law.

193 The amount of photovoltaic generation  $P_s$  is calculated via the model described in [49]

$$P_s = \eta S I_a (1 - 0.005(T_{amb} - 25)) \quad [kWh] \quad (1)$$

194 where  $\eta$  is the conversion efficiency of photovoltaic array (%),  $S$  is the array area ( $m^2$ ),  $I_a$  is the solar  
 195 radiation ( $kW/m^2$ ),  $T_{amb}$  is the outside air temperature ( $^{\circ}C$ ). It is assumed that the total radiation is falling

Table 3: Energy prices

	Grid Energy	Solar Energy	Wind Energy
Price	0.2 €/kWh	0.1 €/kWh	0.05 €/kWh

196 on the photovoltaic array, and the angle of incidence is not considered. Conversion efficiency  $\eta$  is equal  
 197 with 20% which is a typical value for solar arrays and the array area  $S$  is equal with  $200 \text{ m}^2$ . The wind  
 198 turbine produces energy  $P_M$  based on the following equation [50]:

$$P_M = 1/2\rho\pi R^2V^3C_P(\lambda, \beta) \quad [kWh] \quad (2)$$

199 where  $V$  is wind speed in  $[m/s]$ ,  $\rho$  is the air density in  $[kg/m^3]$ ,  $R$  is the blades radius in  $[m]$  and  $C_P$   
 200 the power coefficient. We assume  $\rho = 1.1839kg/m^3$ , the air density at sea level and  $25^\circ C$ ,  $R = 20m$ , and a  
 201 constant  $C_P = 0.4$ , which are the typical values for wind turbines.

202 Finally, the microgrid is equipped with a battery as energy storage: the battery is charged when there is  
 203 excess of energy coming from the renewable resources and discharged when the energy coming from the  
 204 renewable resources is not enough to satisfy the energy demand of the microgrid [51]. The capacity of the  
 205 battery unit is set to  $200 \text{ kWh}$ . However, only 150 out of  $200 \text{ kWh}$  are available for use. That is because, we  
 206 want to avoid discharge greater than 10 % and charge greater than 85 % in order to prologue the life of the  
 207 battery. Thus, in Figure 8, the state of charge of the battery for each scenario is between 10 and 85 %. What  
 208 is more, the rate of charge/discharge was also investigated. Using a 1C charger, and taking into account  
 209 that our battery has a capacity of  $200 \text{ kWh}$ , our system has a capability of charge/discharge rate of  $200 \text{ kW}$ .  
 210 However, in Figure 8, the mean rate of charge between the scenarios is around  $35 \text{ kW}$  and the mean rate of  
 211 discharge is around  $40 \text{ kW}$ . Just once, a peak of  $174 \text{ kW}$  charge rate is developed, but the battery system is  
 212 able to handle it, without wasting any amount energy.

213 The attractiveness of utility-scale energy storage is that it can compensate for the intermittency of wind  
 214 power and solar power. It must be however underlined that in practice large-scale storage technologies other  
 215 than pumped hydro remain in an early stage of development and are expensive [52, 53].

### 216 3. Control objectives

217 One objective of the demand response program is to reduce energy costs: this is achieved if the energy  
 218 available from the renewable sources, which indirectly affects also the energy stored in the storage unit,  
 219 is exploited to the maximum extent. The problem is not trivial since the renewable energy is available  
 220 depending on weather conditions. The wind and solar energy over three different days, depending on wind  
 221 speed and solar radiation respectively, are shown in Figure 3. When the sum of renewable energy and stored  
 222 energy is not enough, extra energy can be absorbed from the main grid. On the other hand, if the energy  
 223 that the renewable sources produce is in excess compared to microgrid energetic needs, the energy is stored  
 224 in the battery; if the storage is at its maximum capacity, the excess of energy is wasted. It is crucial to fully  
 225 take advantage of renewable energy when available in order to enable the ‘islanded mode’ of the microgrid  
 226 and minimize the dependence from the main grid. The demand response is regulated by regulating the  
 227 HVAC operation: the HVAC operation has a direct impact not only on energy demand, but also on the  
 228 thermal comfort of the occupants. If one objective of the demand response program is to reduce energy



229 costs, another objective is to manage the HVAC operation so as to satisfy the thermal comfort of the users.  
 230 The two objectives are expressed by a suitable performance index as explained hereafter.

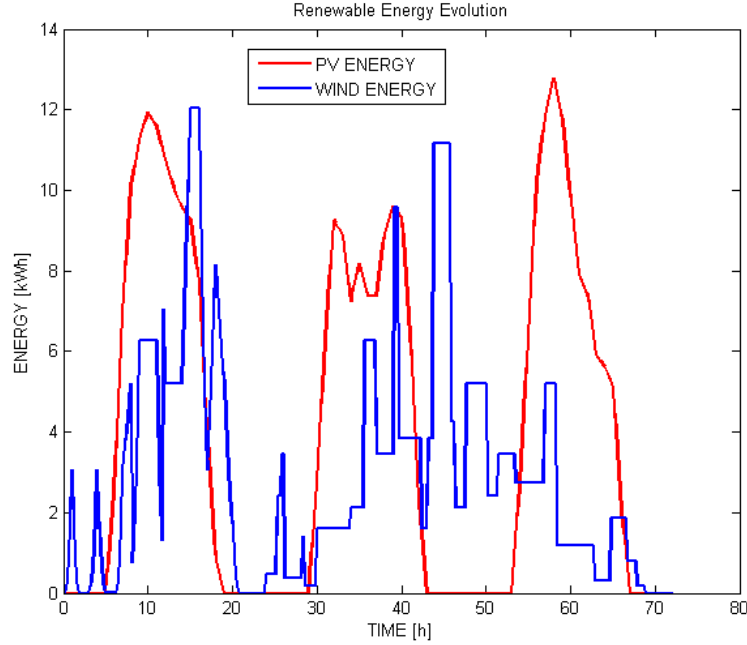


Figure 3: Solar and wind energy evolution over three days

### 231 3.1. Performance Index

232 The performance index to be optimized takes into account two terms: the energy cost and the thermal  
 233 comfort of the occupants. At time  $t$  the aggregate performance index of the three-building microgrid is  
 234 defined as

$$M(t) = \sum_{i=1}^3 (k * E_i(t) + (1 - k) * C_i(t)) \quad (3)$$

235 where  $E_i$  is the energy score and  $C_i$  the thermal comfort score of building  $\#i$ . The energy and the comfort  
 236 score are, typically scaled, so as to be of the same order of magnitude and contribute fairly to the total  
 237 score. According to the importance that the designer wants to give to a term with respect to the other, the  
 238 summation can be weighted using the scaling factor  $0 < k < 1$ .

239 The energy cost includes the price paid for absorbing energy from the main grid, but also the genera-  
 240 tion/maintenance price of renewable energy. The thermal comfort cost we consider is the thermal comfort  
 241 model developed by Fanger [9], which evaluates the Predicted Percentage of Dissatisfied people (PPD) in  
 242 a room. According to the condition of a thermal zone, the thermal comfort is evaluated via a 7-point scale,  
 243 going from -3 (cold) through 0 (neutral) to +3 (hot). Such a scale is called Predictive Mean Vote (PMV).  
 244 The PMV is translated into PPD according to the following formula

$$PPD = 100 - 95e^{-(0.03353PMV^4 + 0.2179PMV^2)} \quad (4)$$

245 According to the ASHRAE 55 standard, the recommended PMV range for thermal comfort is between -  
 246 0.5 and +0.5 for an interior space, which is equivalent to a PPD below 10%. Violation of this bounds are  
 247 accepted but only over short periods of time.

### 248 3.2. Rule-based demand response programs

249 An EnergyPlus model [40, 54] simulates the complex energetic and thermal behavior of each building  
250 composing the microgrid. The implemented demand response program considers the problem of operating  
251 the HVAC during summer, in order to cool-climate the rooms in an energy efficient manner to a user comfort  
252 satisfying level. The operation of the each HVAC unit has one manipulable input that is the temperature set  
253 point (in  $^{\circ}C$ ) with which each unit operates.

254 For comparison reasons, two Rule Based Controllers (RBC) implementing simple but common demand  
255 response programs are adopted. The RBCs employ a simple control strategy, which consists of

- 256 •  $RBC_{24^{\circ}C}$ : keep the HVAC set points of each thermal zone constant to  $24^{\circ}C$  during occupancy hours;
- 257 •  $RBC_{25^{\circ}C}$ : keep the HVAC set points of each thermal zone constant to  $25^{\circ}C$  during occupancy hours;

258 Such control strategies, yet simple, provide acceptable (but far from optimal) performances in terms of the  
259 total score (3). Furthermore, in order to exploit natural ventilation and achieve some energy savings, the  
260 HVAC set point manipulation of  $RBC_{24^{\circ}C}$  and  $RBC_{25^{\circ}C}$  is combined with control of windows. Every time  
261 that HVAC units operate, windows are closed. When the HVAC unit are switched off, the window control  
262 is as follows:

$$\begin{cases} \text{open window} & \text{if } T_{amb} < T_z \text{ and } T_z > 20^{\circ}C \\ \text{close window} & \text{otherwise} \end{cases} \quad (5)$$

263 where  $T_{amb}$  is the outside temperature and  $T_z$  the temperature of the thermal zone. Taking into account  
264 that we want to cool-climate the buildings, the rule in (5) is meant to exploit the natural ventilation effect  
265 occurring typically at night (the room is cooled using the outside temperature). The bound of  $20^{\circ}C$  is set in  
266 order to guarantee a minimum thermal comfort: if the temperature of the room is already below  $20^{\circ}C$  there  
267 is no need to open the window.

268 On the other hand, in order to guarantee the quality of indoor conditions a third window rule is imple-  
269 mented when HVAC are operating. If the internal conditions, and especially the quality of air (big amounts  
270 of humidity) are very low, then windows open, so an external air flow help regulate the conditions inside  
271 the building. Thus, when the HVAC unit are operating, the window control is as follows :

$$\begin{cases} \text{open window} & \text{if } humidity \geq 80 \% \\ \text{close window} & \text{otherwise} \end{cases} \quad (6)$$

272 However, it has to be emphasized that the rule in 6 is never activated in our simulations, meaning that the  
273 HVAC, is never used by the system, as the HVAC manage to keep internal conditions in acceptable levels  
274 during the whole simulation period. *In the setting of this paper interaction between local and aggregate level  
275 occurs via the occupancy schedule: the demand response program should be able to switch off the HVACs  
276 of a building with no occupants, in order to allow the other buildings to use the available renewable energy.*

277 In this section we explained how the emphasis of the work is on joint optimization of energy cost and  
278 thermal comfort. As the microgrid is composed of three buildings, a distinction should be made between  
279 the performance achievable at the building level and the performance achievable at the aggregate level. In  
280 the following section the two levels and their interaction are presented.

## 281 4. Control Strategy

282 In this section, we present the control strategy that it is used in the presented microgrid test case. In  
283 Figure 5, the general form of Supervisory Control Strategy is described. Each buildings, uses its own

284 optimization algorithm (PCAO) and a general node is responsible for the coordination of the different  
 285 buildings.

#### 286 4.1. PCAO Algorithm

287 The problem consists in finding an optimal strategy for the HVAC set points such that the combined  
 288 performance index defined in (3) is minimized. The problem is thus formulated as an optimal control  
 289 problem aiming at minimizing the index

$$J = \int_0^{T_f} \Pi(x(t))dt \quad (7)$$

s.t.

$$\dot{x} = f(x) + Bu, \quad B = [0 \ I]' \quad (8)$$

290 where  $\Pi(\cdot)$  is the analytical expression of the performance index (3), where  $x$  is an augmented, with state  
 291 and control variables, vector of the transformed system dynamics while  $u$  is the time derivative of the actual  
 292 control signals, as demonstrated in 8. The function  $f(x)$  represents the microgrid dynamics, which are  
 293 implemented inside the EnergyPlus model, but that are unknown for our purposes. Finally  $T_f$  is a control  
 294 horizon over which we have reliable weather forecasts (typically 2-3 days). Using dynamic programming  
 295 arguments, we know that the optimal strategy  $u^*$  satisfies the Hamilton-Jacobi-Bellman (HJB) equation

$$\frac{\partial V^*}{\partial x} (f(x) + Bu) + \Pi(x) \quad (9)$$

296 The difficulty in solving the HJB equation in large-scale systems (like our microgrid) was known to Bellman  
 297 itself, which coined the term ‘curse-of-dimensionality’ [55]: in order to overcome such difficulties, the  
 298 PCAO (Parametrized Cognitive Adaptive Optimization) algorithm parametrizes the solution of the HJB  
 299 equation (9) as  $V^*(x) = z'(x)Pz(x)$  and the optimal control strategy via  $u^* = -\frac{1}{2}B'\frac{\partial V^*}{\partial x}$ ,  $P$  is a positive definite  
 300 matrix and  $z(\cdot)$ . More details for the function  $z(\cdot)$  can be found in [56, 57]: in our specific microgrid case we  
 301 found that a linear transformation  $z(x) = x$  is sufficient to achieve important improvements (as demonstrated  
 302 in Section V). With such parametrization, the problem of solving the HJB equation is recast as the problem  
 303 of finding the matrix  $P$  (and thus the strategy  $u$ ) that better approaches the solution of the HJB equation.  
 304 The PCAO algorithm defines the close-to-optimality index (mutated for the principle of optimality [55])

$$\varepsilon(x, P) = V(x(k+1)) - V(x(k)) + \int_k^{k+1} \Pi(x(t))dt \quad (10)$$

305 The solution of the HJB equation (9) brings (10) to zero: the PCAO algorithm, whose steps are presented  
 306 in Figure 4 updates at every time step the strategy parametrized by  $\hat{P}$  in an attempt to minimize the close-  
 307 to-optimality index  $\varepsilon(\hat{P})$  and to make  $\hat{P}$  converge as close as possible to the solution of the HJB equation.  
 308 More about PCAO algorithm can be found in [30, 57, 58]

#### 309 4.2. Feedback vector and Simulation based optimization

310 Each local P-CAO algorithm employs a controller based on a local feedback vectors. The structure of  
 311 each local feedback vector is the following:

- 312 • 3 measurable external weather conditions: outside temperature, outside humidity and solar radiation.
- 313 • 6 forecasts for the mean outside temperature in the next 6 hours.

- 314 • 6 forecasts for the mean solar radiation over the next 6 hours.
- 315 • The  $n$  temperatures of the thermal zones ( $n$  is the number of thermal zones).
- 316 • The  $n$  humidities of the thermal zones.
- 317 • A constant term (since the equilibrium of the system is not in the origin).
- 318 • The  $n$  set points of the HVAC devices in the thermal zones.
- 319 • The  $n$  detectors of occupancy in the thermal zones.

320 Hereafter we explain with more details the choice of the feedback vector: the zone temperature and  
 321 humidities are a natural choice for the thermal state of the building; outdoor weather conditions both in  
 322 the present and the future help to achieve a pro-active control strategy. Finally, the information about the  
 323 occupancy of a thermal zone is provided as a feedback component to the control strategy. The occupancy  
 324 signals are important also for another reason. A frequent problem in building management is the creation  
 325 of comfortable conditions just before people start using the building. In order to achieve this, many control  
 326 strategy uses a training period to "learn" the occupancy schedule. Many smart thermostats available in  
 327 the market employ this mechanism: this is a very useful feature, especially for buildings that are used as  
 328 schools, offices and public offices. Knowing the schedule of occupancy we can change the occupancy  
 329 signals to "on", one hour before the arrival of users in order to create better thermal comfort conditions for  
 330 the people.

331 Using the PCAO algorithm, as presented above, a double feedback loop procedure runs in each build-  
 332 ing (cf. Fig. 4). The primary feedback loop runs in real-time, with actions applied to the actual building  
 333 and measurements collected. In parallel with the primary loop, a secondary simulation-based loop interacts  
 334 with the EnergyPlus model of the building, in order to find better strategies at the next time step. With the  
 335 term 'simulation-based' design we refer to a method where the optimization of the cost function involves  
 336 an iterative process of system simulation/controller redesign. At this point is crucial to introduce and ex-  
 337 plain two time metrics. The control horizon and the simulation horizon. By control horizon we refer to  
 338 the time interval of HVAC management. For example in our test case, the HVAC set points are changed by  
 339 the algorithm every 10 minutes. On the other hand, as a simulation horizon we refer to the whole duration  
 340 of the experiment. Usually, as a simulation horizon we refer to one day or more. This two-loop design is  
 341 implemented in each building separately. The secondary loop, which is implemented based on the Ener-  
 342 gyPlus model, operates in order to find a better controller for the real system. Simultaneously, the primary  
 343 loop/system, uses the best so-far controller to manage the HVAC. The above two-loop procedure can be  
 344 investigated better in Figure 4.

345 **Remark 1.** *The proposed control strategy differs from the classical rolling (or receding) horizon philoso-*  
 346 *phy. In particular, the objective is to update at every time step a feedback controller, rather than solving at*  
 347 *every time step an open loop control problem. After convergence, it was verified via simulations that the*  
 348 *proposed feedback solution provides robustness to the resulting HVAC controller, also in the presence of*  
 349 *different weather conditions than the one used for the design (cf. the results in Table 4). As a result, sim-*  
 350 *ulation results reveal that one can realistically assume keep the same control strategy over long horizons*  
 351 *(indicatively, one week) without the need of redesign the control and without sensible loss of performance.*

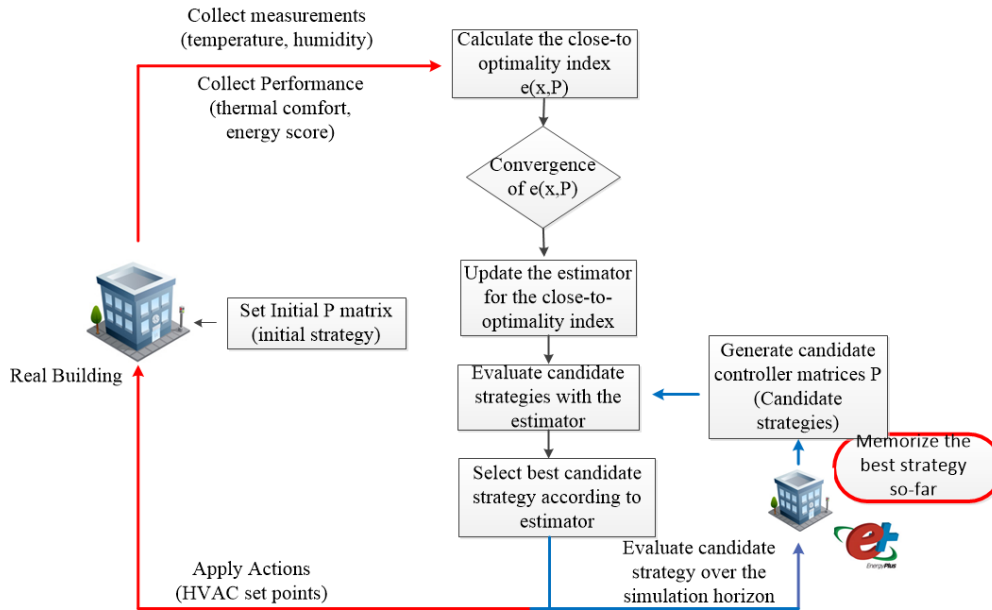


Figure 4: Local simulation-based optimization

### 352 4.3. Supervisory Logic

353 The purpose of this work is to provide a control architecture that that be scalable to an arbitrary number  
 354  $N$  of buildings: for this reason, a centralized control architecture was discarded and the following bi-level  
 355 supervisory strategy was implemented for the control and manipulation of each building/HVAC unit of the  
 356 microgrid. The two levels can be identified as: a *local* building level and an *aggregate* microgrid level.  
 357 In the simulations presented in this work three controllers, one for each building, operate using only local  
 358 information plus information about weather forecast as we described in the sections above. At the aggregate  
 359 level a supervisor takes into account the performance of each building and calculates the total cost, so  
 360 as to optimize the global performance of the microgrid. As compared to a fully centralized strategy, the  
 361 computational and communication requirements of the proposed control architecture are reduced. In Figure  
 362 5 the logic behind the supervisory strategy that we adopt is presented. In each building one local controller  
 363 and one local optimization (PCAO Algorithm) is operated. The goal of each optimization algorithm is to  
 364 optimize the performance of the building by taking into account only local information such as the thermal  
 365 state of the building, occupancy information, and weather conditions. Each local controller communicates  
 366 with the central node and offer information about the cost that the proposed control strategy is achieving and  
 367 achieved in the past. The central node concentrates this information from each different building, calculates  
 368 the total cost and decides if the ‘team’ of controllers achieved the best aggregate performance. The central  
 369 node, informs the local levels with a binary signal, if the the best performance was achieved. Based on  
 370 the Figure 4 the supervisory logic interacts only in the red circle (memorization of the best strategy). As  
 371 a result, the update of the local controller is based on the best global performance rather than on the local  
 372 performance. This simple strategy has been shown to be effective in achieving a good global performance:  
 373 in particular, section V will show that, when a centralized architecture can be implemented, the perfor-  
 374 mance of the centralized and of the proposed supervisory architecture (denoted as Supervisory PCAO) are  
 375 comparable.

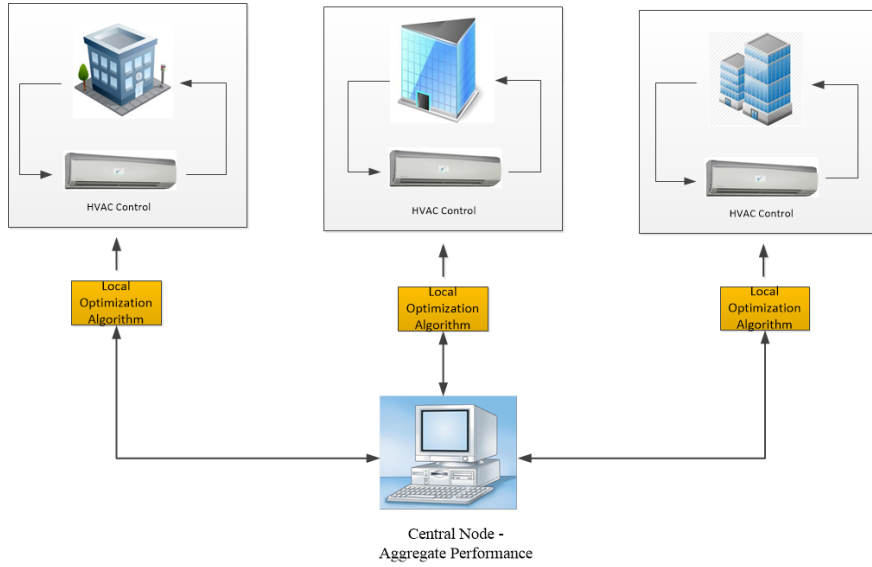


Figure 5: Supervisory control strategy

## 376 5. Simulation Results

377 This section describes the simulation results for the presented microgrid test case. The results of the  
 378 optimization of the demand response and of the thermal comfort achieved via the Supervisory PCAO al-  
 379 gorithm will be compared with the rule-based strategies  $RBC_{24^{\circ}C}$  and  $RBC_{25^{\circ}C}$ , explained in section 3.2.  
 380 Figure 6 shows the energy consumption and occupancy schedule under three control strategies ( $RBC_{24^{\circ}C}$ ,  
 381  $RBC_{25^{\circ}C}$  and PCAO). The distribution of solar and wind energy under the PCAO control strategy is also  
 382 shown (the distribution of renewable energy under  $RBC_{24^{\circ}C}$  and  $RBC_{25^{\circ}C}$  is not shown for better readabil-  
 383 ity of the plots). As mentioned, the renewable energy is distributed proportionally to the energy needs of  
 384 each building. It can be noted how the PCAO algorithm is actively and dynamically managing the demand  
 385 response side via HVAC regulation. It is interesting to note that the PCAO algorithm automatically imple-  
 386 ments the logic of the anticipating the use of HVAC devices some time before the arrival of people (the  
 387 so-called pre-cooling effect). This action leads to the following intelligent behavior: in each building, the  
 388 PCAO energy consumption rises about one hour before people arrive. This might look like a useless waste  
 389 of energy, but it is not, because the comfort index in the PCAO case is relevantly improved over the two  
 390 RBC scenarios. Since the control objective is the optimization of a combined criterion of energy pricing  
 391 and thermal comfort, the overall the total cost is greatly reduced, as the following analysis will reveal.

Table 4: PCAO Improvement (Total Cost) with respect to  $RBC_{24^{\circ}C}$  and  $RBC_{25^{\circ}C}$  (results validated over 7 different sets of 3 days)

Case	Improvement wrt $RBC_{24^{\circ}C}$	Improvement wrt $RBC_{25^{\circ}C}$
Building 1	18-22%	12-17%
Building 2	15-19 %	10-15%
Building 3	19-22 %	13-16%
Microgrid	18-22 %	12-16%

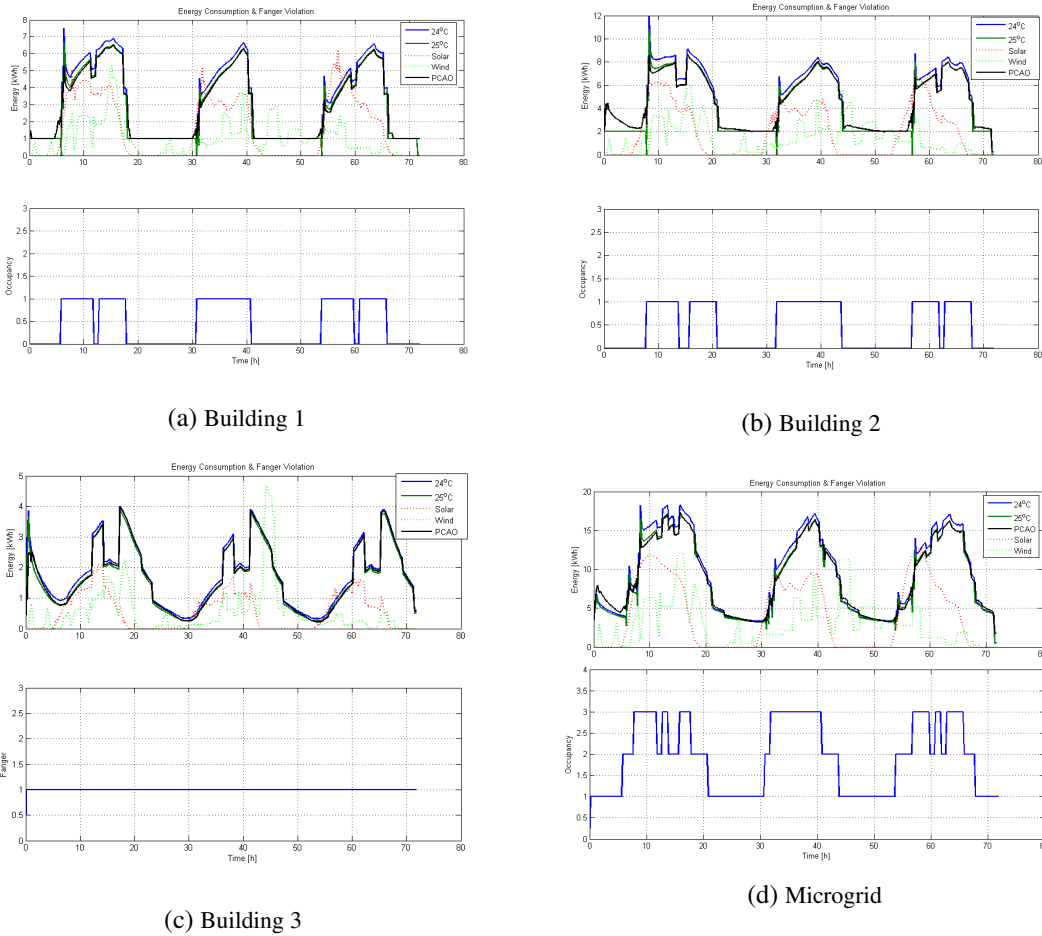


Figure 6: (a)-(b)-(c)-(d): Energy Consumption and Occupancy Schedule during the 3-days, for the three buildings and the whole microgrid test case

392 To evaluate the performance of the whole microgrid system and of its components, we calculate the  
 393 total cost during the entire day. As we mentioned, the total cost consists of the energy cost and thermal  
 394 comfort. Table 4 shows the improvement of PCAO with respect to the 2 rule-based controllers. In each case,  
 395 the Supervisory PCAO strategy attains relevant improvements, ranging from 12 to 22% at the aggregate  
 396 level. The variability arises from the different weather conditions: in fact, the results were validated over 7  
 397 different sets of 3 days, so as to show that the PCAO improvements are consistent in different environmental  
 398 conditions (external temperature, humidity, solar radiation, and wind).

399 In Figure 7, the performance of each 3-day experiment is plotted with respect to energy cost (objective  
 400 1) and thermal comfort (objective 2). The figure proves that PCAO improvements are consistent in different  
 401 conditions and different cases. Furthermore, the figure reveals that PCAO achieves better scores in both  
 402 objectives: it is indeed remarkable to achieve a better thermal comfort while at the same time saving more  
 403 energy. Mathematically, we say that the demand response strategy implemented by PCAO is Pareto optimal  
 404 with respect to the demand response strategy implemented by the two RBCs. In fact, the solutions that  
 405 PCAO offer are much closer to Utopia point than solutions of the other two demand response strategies.  
 406 The Utopia point represents a solution that scores best in both objectives (Energy Cost and PPD), but that it

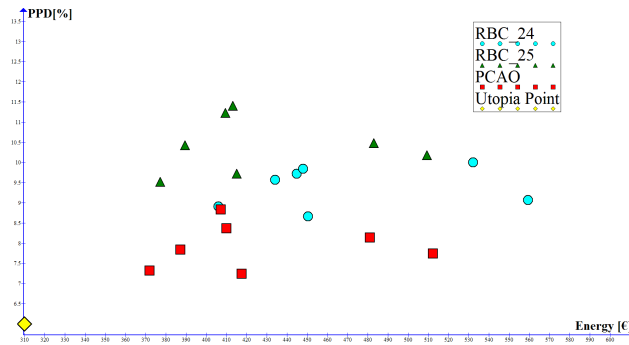


Figure 7: Energy cost (objective 1) and thermal comfort (objective 2) for 7 different experiments of 3 days: it is possible to notice that the 6 points on the extreme right represent very hot experiments where extra energy was required. The Utopia point represents an infeasible performance that cannot be achieved by any demand response strategy.

407 is impossible to reach.

408 To further investigate the PCAO improvements in comparison with the RBC scenarios, three more  
 409 analyzes are presented, which are explained in the following sections.

#### 410 5.1. Use of battery

411 The first analysis regards the use of battery: in Figure 8 and Table 5 the charging/discharging behavior of  
 412 the battery is presented. Both  $RBC_{25^{\circ}C}$  and PCAO algorithm perform better than  $RBC_{24^{\circ}C}$ . In fact,  $RBC_{25^{\circ}C}$   
 413 and PCAO manage to charge the battery to a greater extent, so as to exploit this energy in the evening hours  
 414 when no PV energy is available. Furthermore, PCAO outperforms  $RBC_{25^{\circ}C}$ , as it achieves to charge the  
 415 battery a bit more and use for more time the energy. As a result, less energy from the main grid is absorbed,  
 416 and PCAO manages to exploit better renewable energy resources and achieve better energy pricing. Table 5  
 417 shows to which extent the energy of the battery is better exploited: as compared with  $RBC_{25^{\circ}C}$ , it results that  
 418 PCAO can exploit the battery for 2% more time (around half an hour every day), and the state of charge is  
 419 on average 3% higher (around extra 70 kWh every day).

Table 5: Battery Information

Case	$RBC_{24^{\circ}C}$	$RBC_{25^{\circ}C}$	PCAO
Percentage of usage time	54%	61%	63%
Mean State of charge through experiment	15%	21%	24%

#### 420 5.2. Participation of renewables

421 The second analysis regards the two histograms presented in Figure 9, which have been obtained from  
 422 a 3-day simulation (one of the seven simulation presented above). The first histogram presents the energy  
 423 cost in € for each building and the whole microgrid. The second histogram presents the mean percentage  
 424 of people who are dissatisfied. As already revealed by Figure 7, PCAO achieves better scores in both  
 425 histograms. In particular, with respect to  $RBC_{24^{\circ}C}$ , PCAO manages to save more than 50€ in 3 days for the  
 426 whole system, while maintaining the comfort at better levels (2% better PPD score). On the other hand,



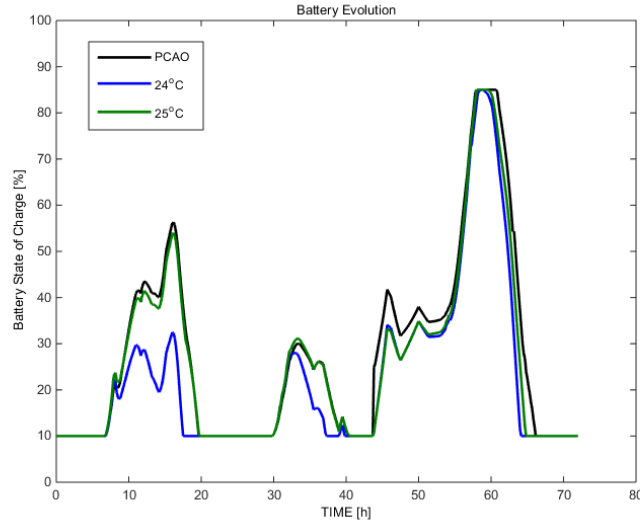


Figure 8: Battery evolution during the 3-day experiment

427 PCAO achieves a slightly better energy cost than  $RBC_{25^{\circ}C}$ : the energy cost is slightly better despite the pre-  
 428 cooling effect implemented by PCAO that demands more energy consumption. Together with improving  
 429 energy cost the PCAO strategy achieves a 3% improvement in PPD as compared with  $RBC_{25^{\circ}C}$ .

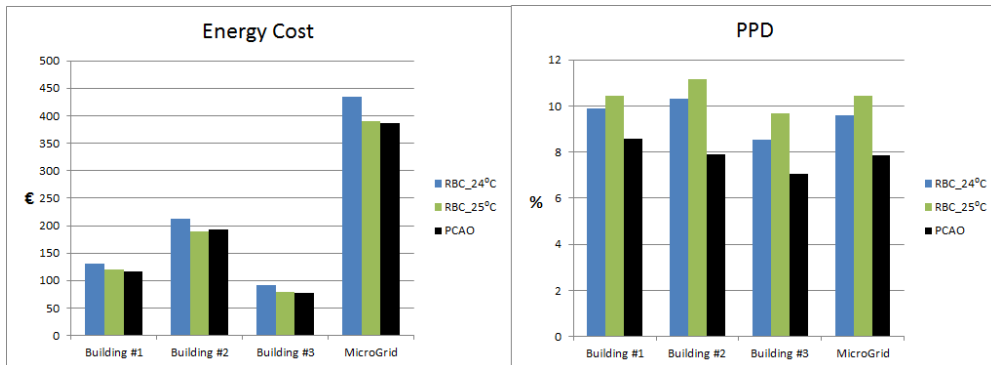


Figure 9: Energy Cost in Euros and Percentage of Dissatisfied People during the 3-day experiment.

430 It is also worth considering how the use of energy is divided among grid and renewable energy under the  
 431 different demand response programs. Figure 10 shows that the percentage of renewable energy is higher in  
 432 the PCAO case. Generally speaking, PCAO strategy achieves to exploit better renewable energy resources  
 433 (and better battery usage), maintain better energy cost levels (even with precooling mode), but without  
 434 sacrificing the comfort levels of users.

### 435 5.3. Robustness of solution-Sensitivity analysis

436 The final analysis is on robustness of the proposed solution: it is well known in control theory that  
 437 a crucial requirement for the design of control strategies is their ability to perform in different conditions  
 438 and show a certain level of robustness and tolerance with respect to changes of system conditions. More

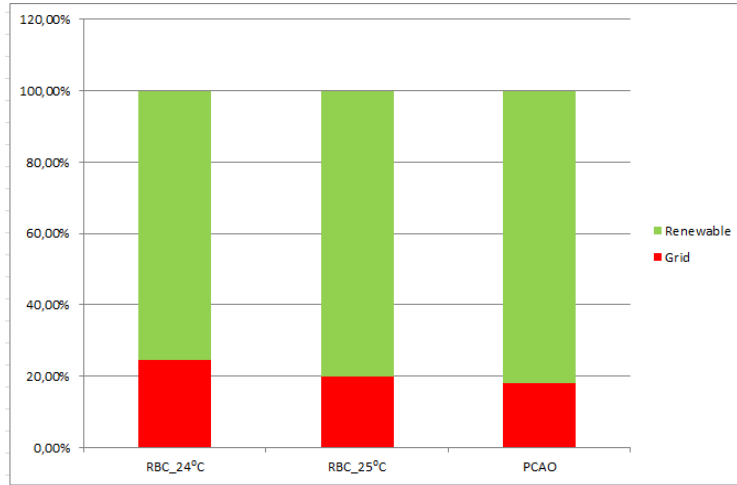


Figure 10: Percentages of Renewable and Grid Energy

439 precisely, the above results were obtained from a control strategy that was optimized over a 3-  
 440 day experiment. Thus, the resulting controller is optimized for the specific three days, with the specific  
 441 occupancy schedule, weather conditions and needs: it is not clear how this controller might perform if tested  
 442 in different days than the ones involved in the optimization step. That is why, in order to test the robustness  
 443 of the proposed method, we tested the controller of the 3-day experiment, *in a 30-day experiment with*  
 444 *different weather conditions and different occupancy schedules.*

Table 6: PCAO Improvement (Total Cost) with respect to  $RBC_{24^{\circ}C}$  and  $RBC_{25^{\circ}C}$  in a 30-day experiment

Case	Improvement wrt $RBC_{24^{\circ}C}$	Improvement wrt $RBC_{25^{\circ}C}$
Building 1	13-16%	8-11%
Building 2	11-14 %	7-9%
Building 3	16-19 %	10-13%
Microgrid	13-17 %	9-11%

445 In Table 6, the numerical results of the 30-day experiment are presented. Obviously, the improvements  
 446 of Table 6, are slightly worse than the improvements of Table 4. However, the degradation of performance  
 447 is acceptable, since the overall improvements range from 9 to 17% (as compared with 12-22% of Table 4).  
 448 This means that a controller optimized over three days can be safely used over much longer horizons: the  
 449 explanation for such a robustness lies in the feedback nature of the PCAO strategy: this is a clear advantage  
 450 over, e.g. receding horizon based demand response programs that require the solution of an optimization  
 451 problem at every time step.

#### 452 5.4. Comparisons against a centralized architecture

453 As a final comparison, the proposed supervisory strategy is compared with a PCAO centralized strategy,  
 454 proposed in [30], using information stemming from the entire microgrid.

455 In Table 7 the comparison between the two strategies is presented. The Centralized-PCAO strategy  
 456 offers better performance than Supervisory-PCAO, but at the expense of slower convergence. It is to be

Table 7: Comparison (Total Cost) between supervisory and centralized PCAO strategy with respect to  $RBC_2$  (results validated over 7 different sets of 3 days)

PCAO-Strategy	Improvement wrt $RBC_2$	Iterations
Supervisory	18-22 %	$\approx 250$
Centralized	22-26 %	$\approx 550$

457 expected that, with data stemming from the entire microgrid, the Centralized-PCAO is not scalable to mi-  
 458 crogrids with an increasing number of buildings. Thus, it is natural to raise concerns about its capability to  
 459 used in bigger problems, with more buildings (50-100). Moreover, as we mentioned earlier, in real cases,  
 460 it is difficult to share private information as the energy-consumption or the demand response with a central  
 461 node or with other partners. On the contrary, the proposed Supervisory strategy, minimize the exchange of  
 462 information and rely heavily on the local optimization algorithms.

## 463 6. Conclusions

464 This paper presented a novel control algorithm for joint demand response management and thermal  
 465 comfort optimization in a microgrid composed of three buildings, a photovoltaic array, a wind turbine, and  
 466 an energy storage unit. The rationale for considering thermal comfort was that comfort plays a major role  
 467 in dynamic demand response, especially in front of intermittent behavior of the renewable energy sources.  
 468 The proposed control strategy adopted a two-level supervisory strategy: at the lower level, each building  
 469 employed a local controller that processes only local measurements; at the upper level, a centralized unit  
 470 supervised and updated the three controllers with the aim of minimizing the aggregate energy cost and  
 471 thermal discomfort of the microgrid. Comparisons with alternative strategies revealed that the proposed  
 472 supervisory strategy efficiently manages the demand response so as to sensibly improve independence of  
 473 the microgrid with respect to the main grid, and guarantees (and improves) at the same time thermal comfort  
 474 of the occupants. The renewable energy sources are fully exploited and better integrated with the main  
 475 grid. Generally speaking, PCAO strategy achieves to exploit better renewable energy resources (and better  
 476 battery usage), maintain better energy cost levels, but without sacrificing the comfort levels of users. The  
 477 improvement are in the range of 12-22%: furthermore, the solution is robust as a controller optimized over  
 478 3 days can be used over much longer horizons (30 days) with improvements in the range 9-17%. Among  
 479 the intelligent behaviors of the proposed strategy are: a pre-cooling action to avoid peaks of discomfort;  
 480 modulation of the HVAC action to avoid peaks of energy consumption; better exploitation of energy from  
 481 the battery; enhanced participation of renewable sources (and thus improved resilience from the grid and  
 482 possibility to enable the islanded mode).

## 483 Acknowledgment

484 The research leading to these results has been partially funded by the European Commission FP7-ICT-  
 485 2013.3.4, Advanced computing, embedded and control systems, under contract #611538 (LOCAL4GLOBAL).

## 486 References

487 [1] Hassan Farhangi. The path of the smart grid. *Power and Energy Magazine, IEEE*, 8(1):18–28, 2010.

- 488 [2] Nikos Hatziaargyriou, Hiroshi Asano, Reza Iravani, and Chris Marnay. Microgrids. *Power and Energy Magazine, IEEE*, 5(4):  
489 78–94, 2007.
- 490 [3] O Alsayegh, S Alhajraf, and H Albusairi. Grid-connected renewable energy source systems: challenges and proposed man-  
491 agement schemes. *Energy Conversion and Management*, 51(8):1690–1693, 2010.
- 492 [4] Robert L Fares and Michael E Webber. Combining a dynamic battery model with high-resolution smart grid data to assess  
493 microgrid islanding lifetime. *Applied Energy*, 137:482–489, 2015.
- 494 [5] Ali Bidram and Ali Davoudi. Hierarchical structure of microgrids control system. *Smart Grid, IEEE Transactions on*, 3(4):  
495 1963–1976, 2012.
- 496 [6] Christopher O Adika and Lingfeng Wang. Smart charging and appliance scheduling approaches to demand side management.  
497 *International Journal of Electrical Power & Energy Systems*, 57:232–240, 2014.
- 498 [7] Luis Pérez-Lombard, José Ortiz, and Christine Pout. A review on buildings energy consumption information. *Energy and*  
499 *buildings*, 40(3):394–398, 2008.
- 500 [8] Liu Yang, Haiyan Yan, and Joseph C Lam. Thermal comfort and building energy consumption implications—a review. *Applied*  
501 *Energy*, 115:164–173, 2014.
- 502 [9] ASHRAE. ANSI/ASHRAE standard 55-2004: thermal environmental conditions for human occupancy. *American Society of*  
503 *Heating, Refrigerating and air-Conditioning Engineers.*, 2004.
- 504 [10] EU Commission et al. Renewable energy road map-renewable energies in the 21st century: building a more sustainable  
505 future. *COM (2006)*, 848, 2007.
- 506 [11] EH Mathews, DC Arndt, CB Piani, and E Van Heerden. Developing cost efficient control strategies to ensure optimal energy  
507 use and sufficient indoor comfort. *Applied Energy*, 66(2):135–159, 2000.
- 508 [12] Mingzhe Liu, Kim Bjarne Wittchen, and Per Kvols Heiselberg. Control strategies for intelligent glazed façade and their  
509 influence on energy and comfort performance of office buildings in denmark. *Applied Energy*, 145:43–51, 2015.
- 510 [13] Zhu Wang, Rui Yang, Lingfeng Wang, RC Green, and Anastasios I Dounis. A fuzzy adaptive comfort temperature model with  
511 grey predictor for multi-agent control system of smart building. In *Evolutionary Computation (CEC), 2011 IEEE Congress*  
512 *on*, pages 728–735. IEEE, 2011.
- 513 [14] M Mossolly, K Ghali, and N Ghaddar. Optimal control strategy for a multi-zone air conditioning system using a genetic  
514 algorithm. *Energy*, 34(1):58–66, 2009.
- 515 [15] C Tzivanidis, KA Antonopoulos, and F Gioti. Numerical simulation of cooling energy consumption in connection with  
516 thermostat operation mode and comfort requirements for the athens buildings. *Applied Energy*, 88(8):2871–2884, 2011.
- 517 [16] Frauke Oldewurtel, David Sturzenegger, and Manfred Morari. Importance of occupancy information for building climate  
518 control. *Applied Energy*, 101:521–532, 2013.
- 519 [17] Xiaohu Xu, Patricia J Culligan, and John E Taylor. Energy saving alignment strategy: achieving energy efficiency in urban  
520 buildings by matching occupant temperature preferences with a buildings indoor thermal environment. *Applied Energy*, 123:  
521 209–219, 2014.
- 522 [18] Andrew Kusiak and Mingyang Li. Optimal decision making in ventilation control. *Energy*, 34(11):1835–1845, 2009.
- 523 [19] Siddharth Goyal, Herbert A Ingle, and Prabir Barooah. Occupancy-based zone-climate control for energy-efficient buildings:  
524 Complexity vs. performance. *Applied Energy*, 106:209–221, 2013.
- 525 [20] G. M. Kopanos, M. C. Georgiadis, and E. N. Pistikopoulos. Energy production planning of a network of micro combined  
526 heat and power generators. *Applied Energy*, 102:1522–1534, 2013.
- 527 [21] Linfeng Zhang, Nicolae Gari, and Lawrence V Hmurcik. Energy management in a microgrid with distributed energy re-  
528 sources. *Energy Conversion and Management*, 78:297–305, 2014.
- 529 [22] T. Broeuer, J. Fuller, F. Tuffner, D. Chassin, and N. Djilali. Modeling framework and validation of a smart grid and demand  
530 response system for wind power integration. *Applied Energy*, 113:199–207, 2014.
- 531 [23] JH Zheng, JJ Chen, QH Wu, and ZX Jing. Multi-objective optimization and decision making for power dispatch of a large-  
532 scale integrated energy system with distributed dhcs embedded. *Applied Energy*, 154:369–379, 2015.
- 533 [24] Elizaveta Kuznetsova, Yan-Fu Li, Carlos Ruiz, and Enrico Zio. An integrated framework of agent-based modelling and robust  
534 optimization for microgrid energy management. *Applied Energy*, 129:70–88, 2014.
- 535 [25] M. Marzband, A. Sumper, A. Ruiz-Alvarez, J. L. Dominguez-Garcia, and B. Tomoiaga. Experimental evaluation of a real  
536 time energy management system for stand-alone microgrids in day-ahead markets. *Applied Energy*, 106:365–376, 2013.
- 537 [26] A. Parisio, E. Rikos, G. Tzamalidis, and L. Glielmo. Use of model predictive control for experimental microgrid optimization.  
538 *Applied Energy*, 115:37–46, 2014.
- 539 [27] Gabriele Comodi, Andrea Giantomassi, Marco Severini, Stefano Squartini, Francesco Ferracuti, Alessandro Fonti, Da-  
540 vide Nardi Cesarini, Matteo Morodo, and Fabio Polonara. Multi-apartment residential microgrid with electrical and thermal  
541 storage devices: Experimental analysis and simulation of energy management strategies. *Applied Energy*, 137:854–866,  
542 2015.
- 543 [28] Xiaohong Guan, Zhanbo Xu, and Qing-Shan Jia. Energy-efficient buildings facilitated by microgrid. *Smart Grid, IEEE*

- 544 *Transactions on*, 1(3):243–252, 2010.
- 545 [29] NZ Azer and S Hsu. The prediction of thermal sensation from a simple model of human physiological regulatory response.  
546 *ASHRAE Trans*, 83(Pt 1), 1977.
- 547 [30] C. D. Korkas, S. Baldi, I. Michailidis, and E. B. Kosmatopoulos. Intelligent energy and thermal comfort management in  
548 grid-connected microgrids with heterogeneous occupancy schedule. *Applied Energy*, 149:194–203, 2015.
- 549 [31] Roberto Z Freire, Gustavo HC Oliveira, and Nathan Mendes. Predictive controllers for thermal comfort optimization and  
550 energy savings. *Energy and buildings*, 40(7):1353–1365, 2008.
- 551 [32] D Kolokotsa, A Pouliezios, G Stavrakakis, and C Lazos. Predictive control techniques for energy and indoor environmental  
552 quality management in buildings. *Building and Environment*, 44(9):1850–1863, 2009.
- 553 [33] Frauke Oldewurtel, Alessandra Parisio, Colin N Jones, Dimitrios Gyalistras, Markus Gwerder, Vanessa Stauch, Beat  
554 Lehmann, and Manfred Morari. Use of model predictive control and weather forecasts for energy efficient building climate  
555 control. *Energy and Buildings*, 45:15–27, 2012.
- 556 [34] Yudong Ma, Francesco Borrelli, Brandon Hency, Brian Coffey, Sorin Benghea, and Philip Haves. Model predictive control  
557 for the operation of building cooling systems. *Control Systems Technology, IEEE Transactions on*, 20(3):796–803, 2012.
- 558 [35] Zhen Yu and Arthur Dexter. Simulation based predictive control of lowenergy building systems using two-stage optimization.  
559 *Proc. IBPSA09*, pages 1562–1568, 2009.
- 560 [36] Truong X Nghiem and George J Pappas. Receding-horizon supervisory control of green buildings. In *American Control  
561 Conference (ACC), 2011*, pages 4416–4421. IEEE, 2011.
- 562 [37] Carina Sagerschnig, Dimitrios Gyalistras, Axel Seerig, Samuel Prívarva, Jiří Cigler, and Zdenek Vana. Co-simulation for  
563 building controller development: The case study of a modern office building. In *Proc. CISBAT*, pages 14–16, 2011.
- 564 [38] Mousa Marzband, Majid Ghadimi, Andreas Sumper, and José Luis Domínguez-García. Experimental validation of a real-  
565 time energy management system using multi-period gravitational search algorithm for microgrids in islanded mode. *Applied  
566 Energy*, 128:164–174, 2014.
- 567 [39] Zhu Wang, Lingfeng Wang, Anastasios I Dounis, and Rui Yang. Multi-agent control system with information fusion based  
568 comfort model for smart buildings. *Applied Energy*, 99:247–254, 2012.
- 569 [40] D. B. Crawley, J. W. Hand, M. Kummert, and B. T. Griffith. Contrasting the capabilities of building energy performance  
570 simulation programs. *Building and environment*, 43(4):661–673, 2008.
- 571 [41] SA Klein. *TRNSYS: A transient simulation program*. Eng. Experiment Station, 1976.
- 572 [42] Ahmed Abdisalaam, Ioannis Lampropoulos, J Frunt, GPJ Verbong, and WL Kling. Assessing the economic benefits of  
573 flexible residential load participation in the dutch day-ahead auction and balancing market. In *European Energy Market  
574 (EEM), 2012 9th International Conference on the*, pages 1–8. IEEE, 2012.
- 575 [43] José Antonio Jardini, Carlos Tahan, MR Gouvea, Se Un Ahn, and FM Figueiredo. Daily load profiles for residential,  
576 commercial and industrial low voltage consumers. *Power Delivery, IEEE Transactions on*, 15(1):375–380, 2000.
- 577 [44] Imene Yahyaoui, Souhir Sallem, MBA Kamoun, and Fernando Tadeo. A proposal for off-grid photovoltaic systems with  
578 non-controllable loads using fuzzy logic. *Energy Conversion And Management*, 78:835–842, 2014.
- 579 [45] Cynthujah Vivekananthan, Yateendra Mishra, Gerard Ledwich, and Fangxing Li. Demand response for residential appliances  
580 via customer reward scheme. *IEEE Trans. Smart Grid*, 5(2):809–820, 2014.
- 581 [46] Wikipedia. Solar power, power cost. [http://en.wikipedia.org/wiki/Solar\\_power#Power\\_cost](http://en.wikipedia.org/wiki/Solar_power#Power_cost), 2014.
- 582 [47] Wikipedia. Wind power, electricity costs and trends. [http://en.wikipedia.org/wiki/Wind\\_power#  
583 Electricity\\_cost\\_and\\_trends](http://en.wikipedia.org/wiki/Wind_power#Electricity_cost_and_trends), 2014.
- 584 [48] Noel Augustine, Sindhu Suresh, Prajakta Moghe, and Kashif Sheikh. Economic dispatch for a microgrid considering renew-  
585 able energy cost functions. In *Innovative Smart Grid Technologies (ISGT), 2012 IEEE PES*, pages 1–7. IEEE, 2012.
- 586 [49] Kenichi Tanaka, Akihiro Yoza, Kazuki Ogimi, Atsushi Yona, Tomonobu Senjyu, Toshihisa Funabashi, and Chul-Hwan Kim.  
587 Optimal operation of dc smart house system by controllable loads based on smart grid topology. *Renewable Energy*, 39(1):  
588 132–139, 2012.
- 589 [50] Yang Peihong, Liu Wenying, and Wei Yili. A survey on problems in smart grid with large capacity wind farm interconnected.  
590 *Energy Procedia*, 17:776–782, 2012.
- 591 [51] Changsun Ahn, Chiao-Ting Li, and Huei Peng. Optimal decentralized charging control algorithm for electrified vehicles  
592 connected to smart grid. *Journal of Power Sources*, 196(23):10369–10379, 2011.
- 593 [52] David Lindley. Smart grids: The energy storage problem. *Nature*, 463(7277):18–20, 2010.
- 594 [53] Ioannis Hadjipaschalis, Andreas Poullikkas, and Venizelos Efthimiou. Overview of current and future energy storage tech-  
595 nologies for electric power applications. *Renewable and Sustainable Energy Reviews*, 13(6):1513–1522, 2009.
- 596 [54] D. B. Crawley, L. K. Lawrie, F. C. Winkelmann, W. F. Buhl, Y. J. Huang, C. O. Pedersen, R. K. Strand, R. J. Liesen, D. E.  
597 Fisher, M. J. Witte, et al. Energyplus: creating a new-generation building energy simulation program. *Energy and Buildings*,  
598 33(4):319–331, 2001.
- 599 [55] Richard Bellman and Robert E Kalaba. *Dynamic programming and modern control theory*. Academic Press New York, 1965.

- 600 [56] Simone Baldi, Iakovos Michailidis, Hossein Jula, Elias B Kosmatopoulos, and Petros A Ioannou. A plug-n-play computa-  
601 tionally efficient approach for control design of large-scale nonlinear systems using co-simulation. In *Decision and Control*  
602 *(CDC), 2013 IEEE 52nd Annual Conference on*, pages 436–441. IEEE, 2013.
- 603 [57] S. Baldi, I. Michailidis, E. B. Kosmatopoulos, and P. A. Ioannou. A plug and play computationally efficient approach for  
604 control design of large-scale nonlinear systems using cosimulation. *IEEE Control Systems Magazine*, 34:56–71, 2014.
- 605 [58] I. Michailidis, S. Baldi, E. B. Kosmatopoulos, and P. A. Ioannou. Adaptive optimal control for large-scale non-linear systems.  
606 *IEEE Transactions of Automatic Control*, page under review, 2014.